Volume 11 | Number 31 | 21 August 2019 | Pages 14475–14962

# Nanoscale

rsc.li/nanoscale

ISSN 2040-3372

ROYAL SOCIETY OF CHEMISTRY | Celebrating IYPT 2019

PAPER
Bethanie J. H. Stadler *et al.*
Nanowarming using Au-tipped $Co_{35}Fe_{65}$ ferromagnetic nanowires

NCNST

Nanoscale

PAPER

View Article Online
View Journal | View Issue



Cite this: *Nanoscale*, 2019, **11**, 14607

# Nanowarming using Au-tipped $Co_{35}Fe_{65}$ ferromagnetic nanowires†

Daniel Shore,[a] Adrian Ghemes,[b] Oana Dragos-Pinzaru,[b] Zhe Gao,[c] Qi Shao,[c] Anirudh Sharma,[c] Joseph Um,[d] Ibro Tabakovic,[d] John C. Bischof[c] and Bethanie J. H. Stadler *[a,d]

Ferromagnetic $Co_{35}Fe_{65}$, Fe, Co, and Ni nanowires have high saturation magnetizations ($M_s$) and magnetic anisotropies, making them ideal for magnetic heating in an alternating magnetic field (AMF). Here, Au-tipped nanowires were coated with polyethylene glycol (PEG) and specific absorption rates (SAR) were measured in glycerol. SAR increased when using metals with increasing $M_s$ ($Co_{35}Fe_{65}$ > Fe > Co > Ni), reaching 1610 ± 20 W $g^{-1}$ metal at 1 mg metal per ml glycerol for $Co_{35}Fe_{65}$ nanowires using 190 kHz and 20 kA $m^{-1}$. Aligning these nanowires parallel to the AMF increased SAR up to 2010 W $g^{-1}$ $Co_{35}Fe_{65}$. Next, $Co_{35}Fe_{65}$ nanowires were used to nanowarm vitrified VS55, a common cryoprotective agent (CPA). Nanowarming rates up to 1000 °C $min^{-1}$ (5 mg $Co_{35}Fe_{65}$ per ml VS55) were achieved, which is 20× faster than the critical warming rate (50 °C $min^{-1}$) for VS55 and other common CPAs. Human dermal fibroblast cells exposed to VS55, and $Co_{35}Fe_{65}$ nanowire concentrations of 0, 1 and 2.5 mg Fe per ml all showed similar cell viability, indicating that the nanowires had minimal cytotoxicity. With the ability to provide rapid and uniform heating, ferromagnetic nanowires have excellent potential for nanowarming cryopreserved tissues.

Received 6th February 2019,
Accepted 3rd May 2019

DOI: 10.1039/c9nr01182j

rsc.li/nanoscale



## 1. Introduction

A significant challenge for organ and tissue transplantation is ischemic injury during the time between removal from the donor and implantation in the recipient.[1] Organs can be preserved by hypothermic storage, for example, hearts can be stored up to 4 hours and kidneys up to 36 hours.[2] To extend this time, tissues and organs can be cryopreserved by vitrification, an approach that converts liquid to glass without crystallization. While there have been recent advances in vitrifying tissues or organs,[3] there are two challenges to successful rewarming of large volumes. First, a rapid heating rate is needed to avoid devitrification, the process of crystallization during warming. For example, one common cryoprotective agent (CPA), VS55, must be heated faster than 50 °C $min^{-1}$,[4] which is its critical warming rate (CWR). Second, uniform heating rates must be achieved throughout the volume to avoid large thermal gradients, which can produce thermal stresses that cause fractures or cracks. Recently, Manuchehrabadi *et al.* used silica–coated iron oxide nanoparticles suspended in VS55 to successfully vitrify and re-warm human dermal fibroblast cells, porcine arteries and porcine aortic heart valve leaflet tissues. Volumes up to 80 ml were placed in a uniform alternating magnetic field (AMF) to heat the nanoparticles by magnetic hysteresis in a process known as nanowarming.[4]

When magnetic nanoparticles (MNPs) are placed in an AMF, they convert the electromagnetic energy into heat through a combination of Neél relaxation and Brownian motion.[5] The heat generated by the MNPs in the AMF increases with the frequency ($f$) and the field strength ($H$).[6] It is also possible to increase the heating efficiency of the MNPs by carefully engineering their shape and material composition.

Indeed, there has been an increasing interest in a variety of MNPs for biomedical applications such as magnetic resonance imaging (MRI) contrast[7] and tumour hyperthermia.[8] The most common MNPs for these applications, are spherical iron oxide nanoparticles.[8] Recently some groups have also investigated the heating properties of magnetic nanorods,[9,10] nanocubes,[9] and nanowires.[11]

[a]*Department of Chemical Engineering & Materials Science, University of Minnesota Twin Cities, Minneapolis, MN 55455, USA. E-mail: stadler@umn.edu*
[b]*National Institute of R&D for Technical Physics, Iasi, Romania*
[c]*Department of Mechanical Engineering, University of Minnesota Twin Cities, Minneapolis, MN 55455, USA*
[d]*Department of Electrical & Computer Engineering, University of Minnesota Twin Cities, Minneapolis, MN 55455, USA*

†Electronic supplementary information (ESI) available. See DOI: 10.1039/c9nr01182j

In an AMF, the energy per gram generated by MNPs in each cycle can be written as:

$$W_{\text{heat}} = \oint H \cdot \mathrm{d}M \quad (1)$$

where $W_{\text{heat}}$ is equal to the area inside the hysteresis loop, $H$ is the applied magnetic field, and $M$ is the magnetization. Fig. 1 shows the full hysteresis loops for Au-tipped 8 μm nickel (Ni) nanowires oriented parallel or perpendicular to an applied magnetic field. The characteristic points are indicated, namely the saturation magnetization ($M_s$), the remnant magnetization ($M_R$) at 0 applied field, the coercive magnetic field ($H_c$) needed to demagnetize the sample, and the anisotropy field ($H_k$) which is the field required to fully align the magnetization in a given direction. For uniaxially anistropic MNPs, the parallel hysteresis loop has an area that has been described[12] as a parallelogram with height = $2(M_s)$ and width = $2(\mu_0 H_k)$, where $\mu_0$ is the permeability of free space. Combining these with the anisotropy energy density:

$$\mu_0 H_k = \frac{2K}{M_s}, \quad (2)$$

the maximum energy per gram is calculated as:

$$W_{\text{heat}}^{\max} = 4 M_s \mu_0 H_k (3).$$

This can be simplified as:

$$W_{\text{heat}}^{\max} = 8K \quad (4)$$

where $K$ is the anisotropy energy density, or the energy required to orient the magnetizations of uniaxial MNPs away from their easy axes.[12]

These equations show that the magnetic anisotropy of the MNPs has an important role in determining the heating properties of the particles. The main sources that contribute to anisotropy energy density for MNP systems are magnetocrystalline anisotropy, shape anisotropy, surface/interface anisotropy, colloidal anisotropy, and magnetoelastic anisotropy. Magnetocrystalline anisotropy is due to the crystal structure dictating a preferred orientation for the atomic magnetic moments relative to the crystallographic axes. Shape anisotropy occurs when the shape of the magnetic material causes a preferred orientation of the magnetic moment with respect to the major/minor axes of the particle to minimize the energy of magnetostatic fields. This is common for high aspect ratio (length: diameter) MNPs that have length ≫ diameter (*e.g.* nanowires, or nanorods). Colloidal anisotropy arises from interactions among magnetic nanoparticles suspended in a liquid that permits the formation of higher order structures, such as chains. If the MNPs are close to each other, then magnetic dipole–dipole interactions between neighboring particles can affect their switching properties. Magnetoelastic anisotropy arises from coupling between strain and magnetization of a magnetic material.

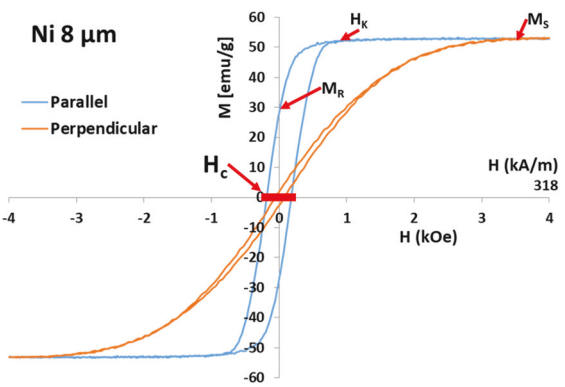


**Fig. 1** Hysteresis loop for 8 μm Ni nanowires aligned in an AAO membrane parallel and perpendicular to the applied field. Red arrows indicate the important magnetic parameters. $H$ is the applied magnetic field and $M$ is the magnetization. Thick red line shows range of field used in SAR measurements.

There have been many studies investigating the heating properties of small, iron oxide MNPs with various shapes and sizes (typically sub-micron), and there have been a few studies using high aspect ratio or high magnetization particles. To compare the heating properties for different MNPs, the specific absorption rate (SAR) is calculated from a plot of temperature *versus* time during heating. Geng *et al.* observed SAR up to 1072 W $g^{-1}$ Fe for $Fe_3O_4$ nanorods (15 nm diameter, 67 nm long at 5 mg $ml^{-1}$).[10] Das *et al.* also studied $Fe_3O_4$ nanorods (5–10 nm diameters, 41–65 nm long) and found SAR up to 862 W $g^{-1}$ Fe (1 mg $ml^{-1}$), with increased SAR for aligned nanorods.[9] Nemati *et al.* achieved SAR of 800 W $g^{-1}$ Fe for $Fe_3O_4$ nanocubes and noted that magnetic anisotropy of the nanoparticles (which depends on their size, shape, arrangement, and dipolar interactions) caused noticeable variations in the SAR.[13] Lin *et al.* measured SAR up to 920.8 W $g^{-1}$ Fe for Fe nanowires (60 nm diameter, 2–6 μm long).[11] Alonso *et al.* found that electrodeposited $Co_{35}Fe_{65}$ nanowires (100 or 300 nm diameter, 2–40 μm long) had high SAR up to 1500 W $g^{-1}$ Fe which increased when the nanowires were aligned parallel with the AMF in agarose.[14] However, these studies used only one nanoparticle concentration, 0.5 mg Fe per ml, which may be too low to provide sufficiently rapid heating of large volumes needed for cryopreservation. One might argue that SAR is in units of W $g^{-1}$, so the same value can be used for higher concentrations, but SAR values typically decrease with higher concentrations.[9–11] This indicates that empirical studies at the desired concentrations are important to demonstrate the feasibility for a specific application. Note, all of the SAR values mentioned above were measured at ~300 kHz AMF, except one at 390 kHz.[9] Therefore, these SAR values would be higher than those of similar MNPs measured at 190 kHz, as shown in this study.

Here, template-assisted electrodeposition[7,15,16] was used to fabricate high $M_s$, high anisotropy magnetic nanowires. One goal was a systematic heating study on the effect of $M_s$, adjusted at 55, 170, 220, and 248 emu $g^{-1}$ by using Ni, Co, Fe, and $Co_{35}Fe_{65}$ nanowires, respectively, with Au tips. The diameter of each nanowire sample (from 10's to 100's of nm) is

 

set by the pore diameter of the anodic aluminium oxide (AAO) that is used as the fabrication template. This study used 200 nm diameter nanowires. The nanowire length is controlled by the electrodeposition time. Both the diameter and length determine the shape anisotropy, which affects the magnetic properties of the nanowires.[17,18] In addition, the nanowires can be coated with PEG or other biological molecules to improve biocompatibility.[15,16] Uncoated metallic nanowires can oxidize in air or water, resulting in reduced magnetization. Therefore, the nanowires used in this work were coated with HS-PEG-COOH on the Au tips, and dopamide-PEG on the $Co_{35}Fe_{65}$, Fe, Co, or Ni surfaces. The hydrophilic PEG can improve the buoyancy and dispersibility of the nanowires by mitigating the magnetic attractive forces between them, see relaxivity measurements in ESI, Table S2.†[19]

This is the first systematic study of Ni, Co, Fe and high $M_s$ $Co_{35}Fe_{65}$ nanowires (200 nm diameter, 0.5–16 μm long) at different concentrations (0.0625–10.0 mg $Co_{35}Fe_{65}$ per ml). The longest, highest aspect ratio nanowires had the highest SAR values for concentrations 1–2 mg $Co_{35}Fe_{65}$ per ml, but at higher concentrations of 5–10 mg $Co_{35}Fe_{65}$ per ml the SAR values were reduced, likely due to increased dipole–dipole interactions, which affected the magnetic switching in the AMF. Aligning the nanowires parallel with the AMF increased the SAR up to 2010 W $g^{-1}$ $Co_{35}Fe_{65}$ for 1 mg $Co_{35}Fe_{65}$ per ml of 8 μm $Co_{35}Fe_{65}$ nanowires aligned in glycerol. After comparing the SAR values for the various nanowires in glycerol, dispersions of nanowires in VS55 were cryogenically vitrified and cooled to −185 °C (using liquid nitrogen vapor). These dispersons were re-warmed in the AMF to simulate nanowarming of cryogenically preserved cells or tissues. Finally, 8 μm $Co_{35}Fe_{65}$ NWs nanowires in VS55 (1 and 2.5 mg Fe per ml) added to human dermal fibroblast (HDF) cells for 3 minutes demonstrated minimal cytotoxicity compared with the VS55 alone. High SAR, fast heating, and low toxicity indicate that magnetic nanowires may be useful for nanowarming.

## 2. Experimental

### a. Nanowire fabrication and coating

Various length $Co_{35}Fe_{65}$ nanowires (1–16 μm) (Fig. 2a, b and ESI Fig. S2†) and 8 μm Co, Fe and Ni nanowires were electrodeposited into 50 μm thick commercial AAO templates (Whatmann Inc. or InRedox). The nominal nanopore diameter was 200 nm. Similar length and diameter nanowires were used by Alonso *et al.*[14] A metallic seed layer of Ti (10 nm) was sputter deposited onto one side of the AAO templates, followed by 400 nm of Cu (either electrodeposited or sputtered) to act as a back-electrode. See ESI Fig. S1† for a diagram depicting NW fabrication steps.

An initial layer of Cu was electrodeposited inside the nanopores and 500 nm Au tips were electrodeposited on both ends of the $Co_{35}Fe_{65}$, Fe, Co, or Ni nanowires. Please refer to ESI S2† for a detailed description of the electrolytes and electrodeposition parameters used. Importantly, $Co_{35}Fe_{65}$ electrodeposited under these conditions has been found to have a high $M_s$ (248 emu $g^{-1}$)[20] while maintaining coercivity.

After electrodepositing the nanowires, the Cu was wet etched using 1.0 M $FeNO_3$. Then, the AAO template was dissolved in 0.7 M $H_3PO_4$ and 0.2 M $CrO_3$ at 80 °C for 60 minutes. The nanowires were magnetically separated and washed 3× with DI water. They were resuspended in 1 ml of 1 mM 2000 MW dopamide-PEG (synthesized using Sigma Aldrich chemicals), and 1 ml of 1 mM SH-PEG-COOH (Sigma Aldrich) for 12 hours to coat the magnetic and Au surfaces, respectively.

### b. Nanowire characterization

The nanowires were imaged while aligned in the AAO template using a Zeiss NEON 40 EsB CrossBeam SEM. The $Co_{35}Fe_{65}$ nanowires had an atomic ratio of Co : Fe = 32 : 68 ± 10%, as determined by EDS. This composition lies in the range of $M_s$ = 248 emu $g^{-1}$ alloys (center value of $Co_{35}Fe_{65}$ according to the Slater Pauling curve), and $M_s$ was confirmed using a Princeton

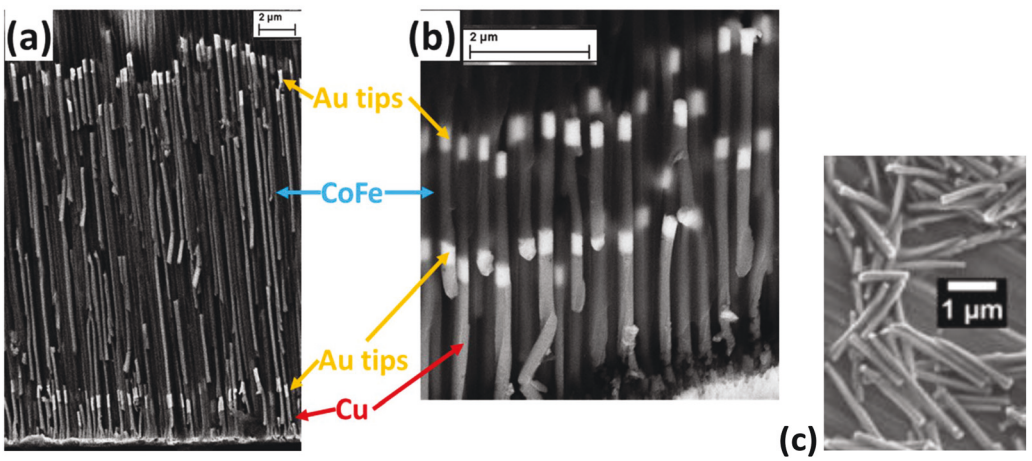


Fig. 2 Cross-sectional SEM images of $Co_{35}Fe_{65}$ nanowires 16 μm (a) and 2 μm (b) aligned in an AAO template. The Cu layers at the bottom were dissolved by 1 M $FeNO_3$ before dissolving the AAO template. Note, some of the NWs were broken when the AAO template was cleaved to make these cross-sectional images. (c) Released Au-tipped Ni nanowires.

vibrating sample magnetometer (VSM). The hysteresis loops of $Co_{35}Fe_{65}$, Fe, Co, and Ni nanowires, (±5 kOe, 25 Oe $s^{-1}$, 25 °C), were measured while they were still inside the AAO, aligned parallel and perpendicular to the applied field. These loops show the extremes of orientation, where random orientations will be between these extremes.

### c. SAR measurements and calculations

To measure and calculate SAR values, nanowire samples in glycerol or VS55 were placed in a 1.7 ml Eppendorf tube and heated using a 1 kW Hotshot inductive heating system with 2.75-turn, water-cooled copper coil, inner diameter 1.75 cm (Ameritherm Inc.). The vial was insulated in styrofoam with sample volumes ranging from 0.1–0.5 ml, depending on the nanowire concentration. The temperature was measured and recorded in one second increments using a Teflon coated fiber-optic temperature probe and Neoptix OptiLink software (Qualitrol Corporation). The time point for 0 seconds on the temperature curve was chosen within the first few seconds after turning on the AMF. For the SAR measurements, the magnetic field amplitude was $H$ = 20 kA $m^{-1}$ (251 Oe) and frequency was $f$ = 190 kHz. For the nanowarming measurements, field amplitudes ($H$ = 20, 25 or 30 kA $m^{-1}$) and frequencies ($f$ = 190 or 360 kHz) were varied, as noted in the text.

### d. Cell viability experiments

For each trial, ~50 000 HDF cells (suspended in cell growth media) were put into one well of a 96 well plate and left overnight to become adherent to the bottom. After 18 hours, the cell growth media was removed, and the cells were loaded with Euro Collins solution, followed by increasing concentrations of VS55 (12.5%, 25%, 50%, 75%) for 3 minutes each. Then, the 75% VS55 was removed and 100 μl of VS55 with 8 μm $Co_{35}Fe_{65}$ nanowires (1 or 2.5 mg $Co_{35}Fe_{65}$ per ml) was added to each well for 3 minutes because cells are typically exposed to liquid VS55 for only 3 minutes during nanowarming. Next, the nanowire suspension was removed, and the cells were rinsed with decreasing concentrations of VS55 until they were fully loaded with Euro Collins solution, as before. Finally, the cells were stained with using a Hoechst-PI double stain and imaged using a fluorescent microscope to count the living and dead cells, $N$ >200 cells per sample.

## 3. Results and discussion

First, the impact of $M_s$ on heating was studied. 8 μm long $Co_{35}Fe_{65}$, Fe, Co and Ni nanowires were mixed in glycerol at various concentrations and placed in the AMF ($H$ = 20 kA $m^{-1}$, or 251 Oe, $f$ = 190 kHz). The SAR values were calculated using the Box–Lucas curve-fitting method, where eqn (5) is used to calculate parameters $A$ and $\lambda$, which are then used to calculate SAR with eqn (6):

$$\Delta T = A(1 - e^{-\lambda t}) \quad (5)$$

$$\mathrm{SAR} = \frac{A\lambda C}{m_{\mathrm{MNP}}} \quad (6)$$

The Box–Lucas method was used because it is reliable to calculate the SAR for non-adiabatic systems such as this.[21] The curve fitting was done for the first 180 seconds of the heating measurements, Fig. S3 in ESI,† and $C$ is the heat capacity of glycerol (3.04 J $ml^{-1}$ $K^{-1}$).

Fig. 3a shows that the highest $M_s$ metal ($Co_{35}Fe_{65}$) had the highest SAR values, and SAR decreased as materials with lower $M_s$ were used (Fe, Co, and Ni, respectively). Fig. 3b, c and d show the parallel and perpendicular hysteresis loops for the $Co_{35}Fe_{65}$, Fe, Co nanowires, while Ni is shown in Fig. 1. The $M_s$ values are similar to the bulk values for each metal ($Co_{35}Fe_{65}$ 248 emu $g^{-1}$, Fe 218 emu $g^{-1}$, Co 161 emu $g^{-1}$, Ni 54.4 emu $g^{-1}$).[20,22] Although SAR monotonically increased with the $M_s$ of the nanowire materials, the relationship was not linear for several reasons. First, Fe nanowires had lower relative SAR because Fe readily oxidizes, which can lead to canted magnetic moments and iron oxides on the surfaces, both of which lower $M_s$.[23] For reference, iron oxide exists in many forms with $M_s$ of 0 (hematite) to 87 (magnetite) emu $g^{-1}$. Co nanowires also had lower relative SAR values, most likely because Co has 10× higher crystallographic anisotropy than the other metals which may be competing with the nanowire shape anisotropy, leading to a sheared hysteresis loop[24] (Fig. 3d). This shearing reduces the area of the loop, and therefore reduces heating.

Dipole interactions between neighbouring nanowires also affect the switching of the magnetic domains.[25] The dipole interactions become more noticeable at higher nanowire concentrations because the nanowires are closer together. This could explain why the SAR values are typically higher at lower concentrations in literature[8–10] and in every curve in Fig. 3a. See a comparison of 0.125 and 0.25 mg $Co_{35}Fe_{65}$ per ml in ESI Fig. S4.† For the same size nanowire, 10× increase in concentration will lead to a cubed root of 10 (or 2.15×) closer spacing ($r$). Since dipole fields are proportional to $r^{-3}$, this can be a significant effect that increases further as spacing becomes similar in size as the nanowire dimensions.

The nanowires have a lower saturation field when they are aligned parallel with the field, which means a lower magnetic field is needed to completely flip the magnetizations. Therefore, the nanowires should generate more heat in lower magnetic fields with the nanowires aligned parallel with the AMF rather than perpendicular or randomly oriented.[26,27] This is especially useful for heating biological tissues, for which it is preferable to use lower AMFs to avoid strong eddy currents.

Given the successful heating with the high-$M_s$ $Co_{35}Fe_{65}$ nanowires, this material was used for the remainder of the paper. First, a study was conducted to measure how the nanowire length affects SAR values at different concentrations, Fig. 4a. In general, the SAR values increased with increasing nanowire length, which agrees with the SAR trend observed by Alonso *et al.*[14] As the nanowire length increases, the magnetic anisotropy also increases because the demagnetization factor is larger for longer magnetic domains. However, longer nanowires

 

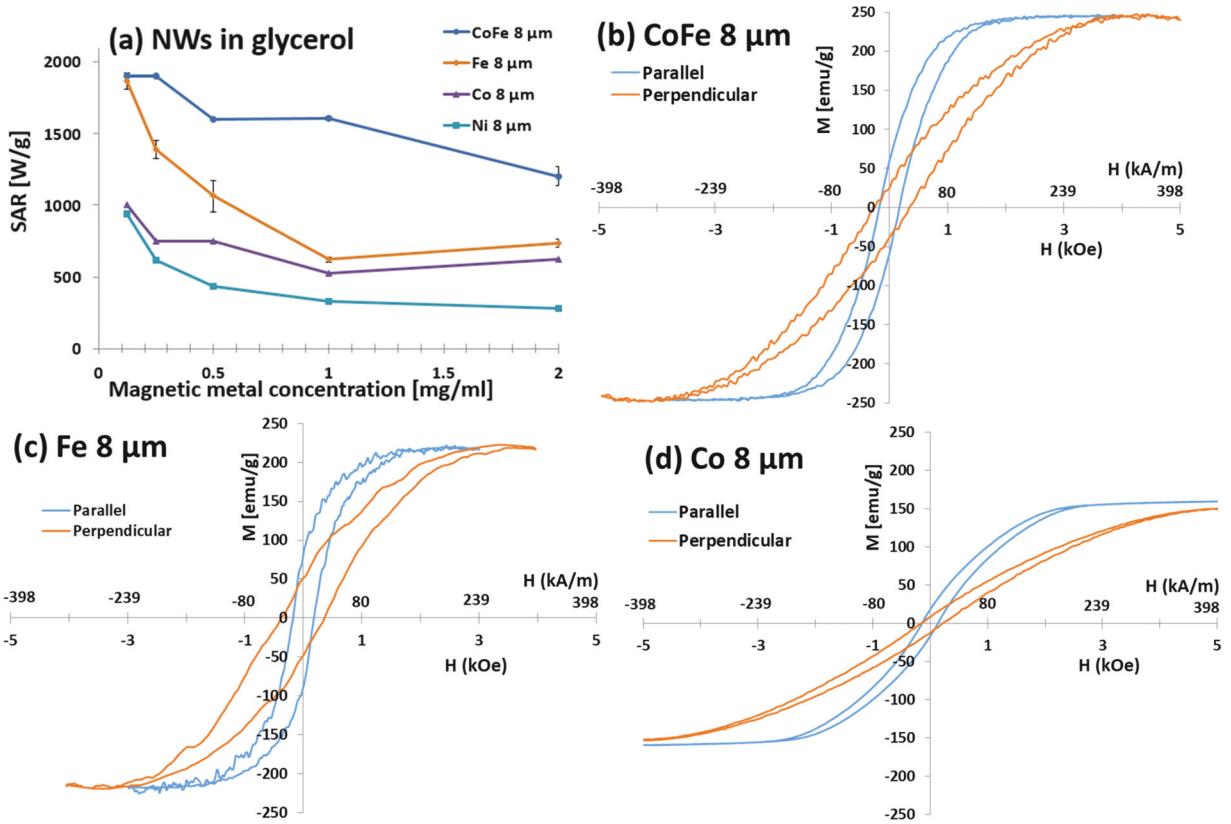


Fig. 3 (a) SAR values for nanowires with different $M_s$ in glycerol at various concentrations using 20 kA m$^{-1}$. Hysteresis loops for 8 µm (b) $Co_{35}Fe_{65}$, (c) Fe, and (d) Co nanowires aligned in AAO membranes parallel and perpendicular to the applied field. Note, 1 kOe = 79.6 kA m$^{-1}$ and the thick red line shows the strength of the field for SAR measurements.

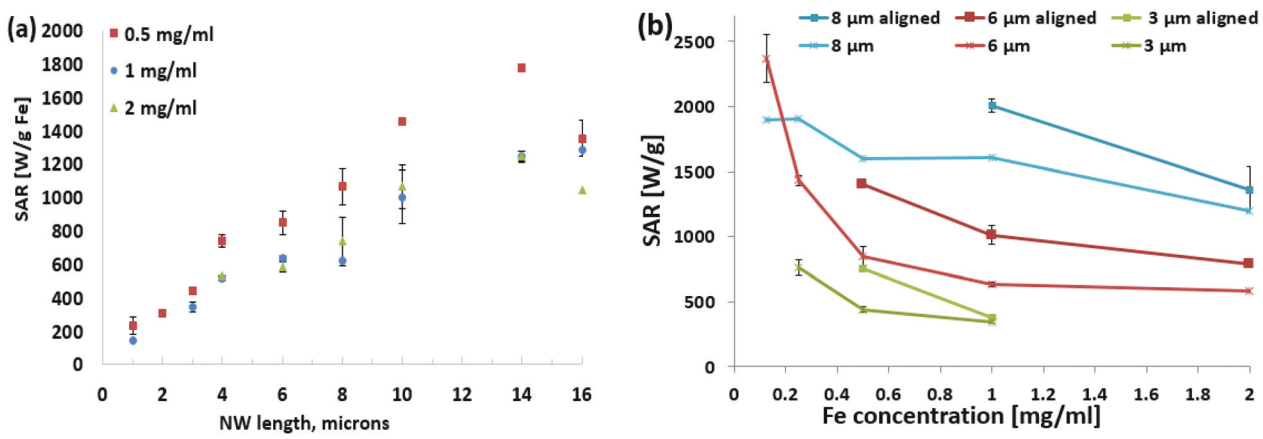


Fig. 4 (a) SAR values for different length $Co_{35}Fe_{65}$ nanowires in glycerol at various concentrations. (b) Graph showing the SAR values for different lengths and alignment of $Co_{35}Fe_{65}$ nanowires in glycerol at various concentrations. The asterisk marker indicates the nanowires were randomly oriented while the square marker indicates the nanowires were aligned parallel to the AMF before heating to show effect of particle anisotropy on heating.

can have multiple magnetic domains so the magnetic domain length does not continue increasing with the nanowire length.

As with Fig. 3a, the SAR values were higher for lower concentrations for all the different length $Co_{35}Fe_{65}$ nanowires (ESI Fig. S4†). Lin *et al.* also observed increasing SAR values for iron nanowires at lower concentrations (0.1 mg ml$^{-1}$) for 2–6 µm long Fe nanowires.[11] As before, this is likely because the nanowires have fewer dipole interactions at lower concentrations, because they are farther apart from each other.[25] For 16 µm nanowires, which have larger magnetic dipole fields,

the average center–center spacing is 32 μm at 0.125 mg ml$^{-1}$ and only 7.6 μm (~38 diameters) at 10 mg ml$^{-1}$.

Although the SAR values are higher at low concentrations, the temperature increase per minute is smaller because the nanowire mass is smaller. It would be difficult to achieve the rapid heating rates (above CWR) needed to re-warm vitrified samples. Encouragingly these SAR values were similar to those observed by Alonso *et al.*,[14] which is the only previous group to report SAR values for electrodeposited $Co_{35}Fe_{65}$ nanowires. They used $H$ = 23.9 kA m$^{-1}$ and $f$ = 310 kHz.

Glycerol was used for these heating experiments because it has a higher viscosity and density than water, with a lower $C_p$. The high-viscosity glycerol prevented the nanowires from settling to ensure a uniform concentration during heating. It also restricted the rotational movement of the nanowires in the 190 kHz AMF. This motion-restricting environment is similar to having nanowires dispersed in a cooled or vitrified cryoprotective agent. With the nanowires suspended in glycerol, they were aligned by placing the sample in a uniform DC magnetic field ($H$ = 1.6 kA m$^{-1}$) generated by a Helmholtz coil (750 turns) and a 3-amp DC power supply (ESI Fig. S6†).

Heating curves were measured for several samples with the nanowires aligned parallel to the AMF prior to measurement, Fig. 4b. SAR increased for all of the aligned samples. For the 8 μm $Co_{35}Fe_{65}$ nanowires the SAR increased from 1610 W g$^{-1}$ $Co_{35}Fe_{65}$ (randomly oriented) to 2010 W g$^{-1}$ $Co_{35}Fe_{65}$ for aligned nanowires. Alonso *et al.* also observed an increase in SAR values with $Co_{35}Fe_{65}$ nanowires aligned with the magnetic field.[14] These experimental results agree nicely with the magnetic hysteresis data in Fig. 3b. When the nanowires are aligned parallel to each other and the AMF (instead of randomly oriented), they have a lower saturation field. Even below saturation, it is obvious from Fig. 3b that parallel loops have more area, and therefore better heating at ±20 kA m$^{-1}$. This point is further illustrated below.

Because cryogenic nanowarming typically requires high concentrations (>2 mg Fe per ml) to achieve high heating rates, two higher concentration nanowire samples were measured in glycerol. Fig. 5a shows that nanowire alignment increased SAR values at 2 mg ml$^{-1}$ and 5 mg ml$^{-1}$. At 10 mg ml$^{-1}$ the SAR values were similar for aligned or random nanowires. Presumably, the dipole fields of the nanowires interact at such a high concentration.

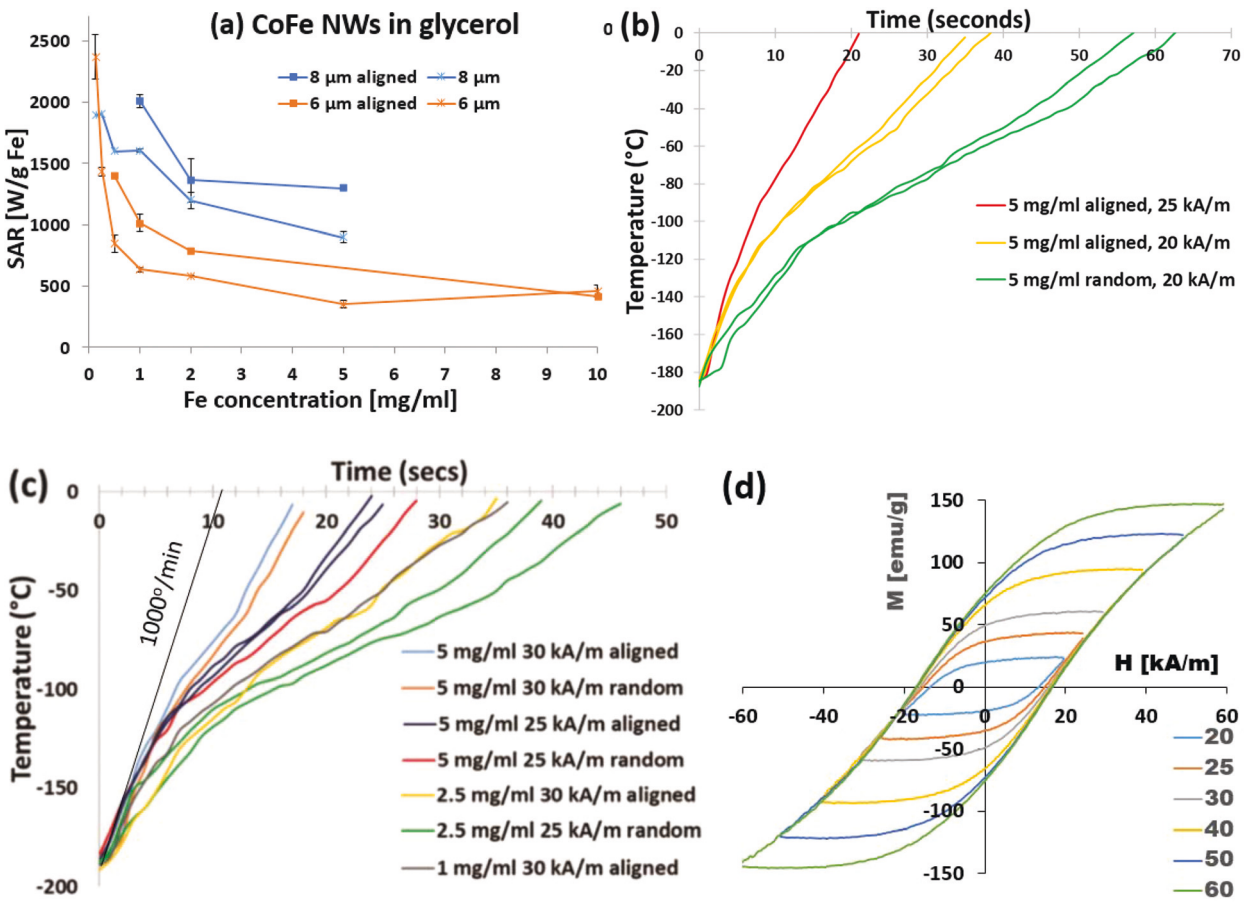


**Fig. 5** (a) SAR values for 6 and 8 μm $Co_{35}Fe_{65}$ nanowires in glycerol at various concentrations, with the nanowires randomly oriented or aligned parallel to the AMF. (b) Heating curves for 8 μm $Co_{35}Fe_{65}$ nanowires (5 mg ml$^{-1}$) in VS55 at 360 kHz and 20 or 25 kA m$^{-1}$. (c) Heating curves for 8 μm $Co_{35}Fe_{65}$ nanowires at 1, 2.5, or 5 mg $Co_{35}Fe_{65}$ per ml at 25 or 30 kA m$^{-1}$ with the nanowires randomly oriented or aligned parallel to the AMF. (d) Minor hysteresis loops of 8 μm $Co_{35}Fe_{65}$ nanowires aligned in an AAO membrane parallel to the applied field. Minor loops with nanowires perpendicular to the applied field are in ESE (Fig S5d†). Repeated colors in (b) and (c) are repeated measurements.

$Co_{35}Fe_{65}$ nanowires were dispersed in a standard cryopreservation agent, VS55, at concentrations of 1, 2.5, 5, and 10 mg $Co_{35}Fe_{65}$ per ml. Fig. 5b shows the heating curves for 8 μm $Co_{35}Fe_{65}$ nanowires (5 mg $ml^{-1}$) heated in VS55 at 20 kA $m^{-1}$ and 360 kHz, with or without magnetic alignment. The nanowires heated at least an order of magnitude above the CWR for VS55 (50 °C $min^{-1}$) and much faster than commercial Ferrotec iron oxide particles coated with mesoporous silica.[4] This is expected, since these $Co_{35}Fe_{65}$ nanowires have more area inside their hysteresis loops, and therefore higher SAR values than the iron oxide particles.[28] When the AMF was increased to 25 kA $m^{-1}$, with the nanowires aligned, the heating rate increased even more. After this intriguing result, several different combinations of concentration (1, 2.5, 5, or 10 mg Fe per ml), AMF (25 or 30 kA $m^{-1}$), and nanowire alignment were tested, with the results in Fig. 5c. All of these combinations resulted in fast initial heating rates, up to 1000 °C $min^{-1}$ for aligned 5 mg $Co_{35}Fe_6$ per ml and for 10 mg $Co_{35}Fe_{65}$ per ml (ESI Fig. S7†). The dramatic increase in heating rates with the AMF at 25 or 30 kA $m^{-1}$, can be easily explained using the minor hysteresis loops, Fig. 5d. The magnetization of the $Co_{35}Fe_{65}$ nanowires aligned in an AAO membrane parallel to the applied field increased by increasing the AMF from ±20 to ±60 kA $m^{-1}$ (±0.25, to ±0.75 kOe). Therefore, the area inside of the minor loops increased as the sample magnetization approached saturation (from Fig. 3b, $H_k$ = 200 kA $m^{-1}$, or 2.5 kOe). A similar family of loops for Fe, Co, and Ni nanowires are shown in ESI Fig. S5,† and to further demonstrate anisotropy, the minor loops of $Co_{35}Fe_{65}$ nanowires perpendicular to the field are shown in ESI Fig. S5d.† The 1 kW heating coil cannot achieve AMFs above 30 kA $m^{-1}$; however, larger 15 kW systems can achieve fields as high as 60 kA $m^{-1}$ which would be useful to nanowarm larger volumes.[4] With higher AMFs, there may be a safety concern due to eddy currents. However, the AMF can be turned off once the sample reaches −20 °C to avoid damaging the tissues or cells, or a lower frequency can be used.

Importantly, the $Co_{35}Fe_{65}$ nanowires achieved heating at 256 °C $min^{-1}$ using only 1 mg $Co_{35}Fe_{65}$ per ml. This means the nanowires could potentially be used for nanowarming with only a fraction of the MNP mass required for typical iron oxide particles (10 mg Fe per ml).[4] These results demonstrate that the nanowire heating rates can be tuned depending on the concentration and the AMF strength, which offers useful flexibility to achieve rapid heating rates in larger volumes for tissues or organs.

After successfully demonstrating the heating rates in vitrified VS55, the cytotoxicity of the PEG coated $Co_{35}Fe_{65}$ nanowires in VS55 at 4 °C was measured using HDF cells. HDF cells in cell culture medium exposed to a 25 or 30 kA $m^{-1}$ AMF for 3 minutes had similar viability as cells with no AMF exposure (Fig. 6a). These results indicate that $Co_{35}Fe_{65}$ nanowires with a 25 or 30 kA $m^{-1}$ AMF will not be harmful in nanowarming cells or tissues. HDF cells had similar viability in VS55 with 0, 1, or 2.5 mg $Co_{35}Fe_{65}$ per ml of 8 μm $Co_{35}Fe_{65}$ nanowires (Fig. 6(b)). Note that VS55 can be toxic to the cells, especially above −20 °C, so exposure was limited to 3 minutes, as it would be during nanowarming procedures.

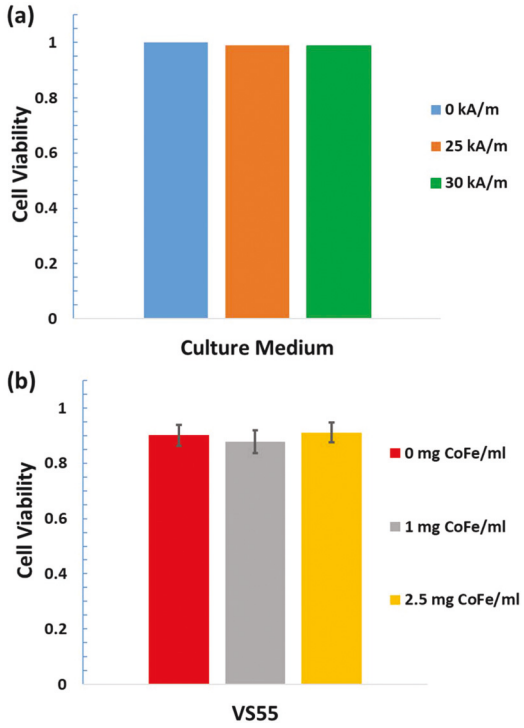


**Fig. 6** Viability of HDF cells. (a) Cells with no nanowires in cell culture medium with AMF 0, 25, or 30 kA $m^{-1}$, for 3 minutes. (b) Cells in VS55 with 0, 1 or 2.5 mg $Co_{35}Fe_{65}$ per mL of nanowires without AMF. Cell viability was tested after the complete removal of VS55 and/or $Co_{35}Fe_{65}$ nanowires.

## 4. Conclusions

High moment Au-tipped nanowires were explored for potential as nanowarming agents. First, $Co_{35}Fe_{65}$, Fe, Co, and Ni nanowires were dispersed in glycerol to inhibit nanowire motion during heating studies in an alternating magnetic field (AMF). They were found to have SAR values that decreased monotonically with their magnetizations (248, 220, 170, and 55 emu $g^{-1}$, respectively). This was explained by a reduction in the area of the hysteresis loop since the height of the loop is 2× $M_s$ and the width is proportional to 2× the coercivity, $H_c$. Hysteresis loops were measured for the extremes of orientation (parallel and perpendicular to the applied field), and parallel orientations reached saturation at significantly lower fields. Subsequently $Co_{35}Fe_{65}$ nanowires were oriented parallel to the AMF (190 kHz, 20 kA $m^{-1}$), which led to an increase from 1610 (random) to 2010 (aligned) ±20 W $g^{-1}$ $Co_{35}Fe_{65}$ at 1 mg metal per ml glycerol for 8 μm-long $Co_{35}Fe_{65}$ nanowires. Minor loops were also measured to show the increase in area obtained by increasing the AMF from 20 to 60 kA $m^{-1}$. All of these studies were done from room temperature. Next, Au-tipped $Co_{35}Fe_{65}$ nanowires were frozen in vitrified VS55, both randomly

oriented and aligned parallel to the AMF. Very fast initial heating 1000 °C $min^{-1}$ was obtained for aligned nanowires, which is 20× higher than the critical warming rates (~50 °C $min^{-1}$) of most cryopreservation agents. These promising thermal results indicate that nanowires have excellent potential as nanowarming agents. Cell toxicity in the presence of the nanowires was confirmed to be minimal, and the door is open for future tissue warming studies.

## Conflicts of interest

There are no conflicts to declare.

## Acknowledgements

Portions of this work were conducted in the Minnesota Nano Center and Characterization Facility, which are supported by the National Science Foundation through the National Nano Coordinated Infrastructure Network (NNCI) under Award Number ECCS-1542202. This work was also supported by the National Science Foundation (ECCS 1509543), the Romanian Ministry of Research and Innovation (Projects PN 18 06 01 01 and PN 19 28 01 01), and the National Institute of Health (5R01DK117425-02 and 5R01HL135046-02).

## Notes and references

1 S. Giwa, J. K. Lewis, L. Alvarez, R. Langer, A. E. Roth, G. M. Church, J. F. Markmann, D. H. Sachs, A. Chandraker, J. A. Wertheim and M. Rothblatt, The promise of organ and tissue preservation to transform medicine, *Nat. Biotechnol.*, 2017, **35**(6), 530–542.

2 J. K. Lewis, J. C. Bischof, I. Braslavsky, K. G. M. Brockbank, G. M. Fahy, B. J. Fuller, Y. Rabin, A. Tocchio, E. J. Woods, B. G. Wowk, J. P. Acker and S. Giwa, The Grand Challenges of Organ Banking: Proceedings from the first global summit on complex tissue cryopreservation, *Cryobiology*, 2016, **72**(2), 169–182.

3 K. G. M. Brockbank, Z. Z. Chen, E. D. Greene and L. H. Campbell, Vitrification of Heart Valve Tissues, *Cryopreservation and Freeze- Drying Protocols*, 3rd edn, 2015, vol. 1257, pp. 399–421.

4 N. Manuchehrabadi, Z. Gao, J. J. Zhang, H. L. Ring, Q. Shao, F. Liu, M. McDermott, A. Fok, Y. Rabin, K. G. M. Brockbank, M. Garwood, C. L. Haynes and J. C. Bischof, Improved tissue cryopreservation using inductive heating of magnetic nanoparticles, *Sci. Transl. Med.*, 2017, **9**(379), eaah4586.

5 R. E. Rosensweig, Heating magnetic fluid with alternating magnetic field, *J. Magn. Magn. Mater.*, 2002, **252**(1–3), 370–374.

6 R. Hergt and S. Dutz, Magnetic particle hyperthermia-biophysical limitations of a visionary tumour therapy, *J. Magn. Magn. Mater.*, 2007, **311**(1), 187–192.

7 D. Shore, S. L. Pailloux, J. Zhang, T. Gage, D. J. Flannigan, M. Garwood, V. C. Pierre and B. J. H. Stadler, Electrodeposited Fe and Fe-Au nanowires as MRI contrast agents, *Chem. Commun.*, 2016, **52**(85), 12634–12637.

8 S. Tong, C. A. Quinto, L. L. Zhang, P. Mohindra and G. Bao, Size-Dependent Heating of Magnetic Iron Oxide Nanoparticles, *ACS Nano*, 2017, **11**(7), 6808–6816.

9 R. Das, J. Alonso, Z. N. Porshokouh, V. Kalappattil, D. Torres, M. H. Phan, E. Garaio, J. A. Garcia, J. L. S. Llamazares and H. Srikanth, Tunable High Aspect Ratio Iron Oxide Nanorods for Enhanced Hyperthermia, *J. Phys. Chem. C*, 2016, **120**(18), 10086–10093.

10 S. Geng, H. T. Yang, X. Ren, Y. H. Liu, S. L. He, J. Zhou, N. Su, Y. F. Li, C. M. Xu, X. Q. Zhang and Z. H. Cheng, Anisotropic Magnetite Nanorods for Enhanced Magnetic Hyperthermia, *Chem. – Asian J.*, 2016, **11**(21), 2996–3000.

11 W. S. Lin, H. M. Lin, H. H. Chen, Y. K. Hwu and Y. J. Chiou, Shape Effects of Iron Nanowires on Hyperthermia Treatment, *J. Nanomater.*, 2013, 237439.

12 C. L. Dennis and R. Ivkov, Physics of heat generation using magnetic nanoparticles for hyperthermia, *Int. J. Hyperthermia*, 2013, **29**(8), 715–729.

13 Z. Nemati, J. Alonso, I. Rodrigo, R. Das, E. Garaio, J. A. Garcia, I. Orue, M. H. Phan and H. Srikanth, Improving the Heating Efficiency of Iron Oxide Nanoparticles by Tuning Their Shape and Size, *J. Phys. Chem. C*, 2018, **122**(4), 2367–2381.

14 J. Alonso, H. Khurshid, V. Sankar, Z. Nemati, M. H. Phan, E. Garayo, J. A. Garcia and H. Srikanth, FeCo nanowires with enhanced heating powers and controllable dimensions for magnetic hyperthermia, *J. Appl. Phys.*, 2015, **117**(17), 17D113.

15 A. Sharma, G. M. Orlowski, Y. Zhu, D. Shore, S. Y. Kim, M. D. DiVito, A. Hubel and B. J. H. Stadler, Inducing cells to disperse nickel nanowires via integrin-mediated responses, *Nanotechnology*, 2015, **26**(13), 135102.

16 A. Sharma, Y. Zhu, S. Thor, F. Zhou, B. Stadler and A. Hubel, Magnetic Barcode Nanowires for Osteosarcoma Cell Control, Detection and Separation, *IEEE Trans. Magn.*, 2013, **49**(1), 453–456.

17 S. M. Reddy, J. J. Park, S.-M. Na, M. M. Maqableh, A. B. Flatau and B. J. H. Stadler, Electrochemical Synthesis of Magnetostrictive Fe-Ga/Cu Multilayered Nanowire Arrays with Tailored Magnetic Response, *Adv. Funct. Mater.*, 2011, **21**(24), 4677–4683.

18 S. M. Reddy, J. J. Park, M. M. Maqableh, A. B. Flatau and B. J. H. Stadler, Magnetization reversal mechanisms in 35 nm diameter Fe1-xGax/Cu multilayered nanowires, *J. Appl. Phys.*, 2012, **111**(7), 3.

19 A.-H. Lu, E. L. Sabalas and F. Schuth, Magnetic Nanoparticles: Synthesis, Protection, Functionalization, and Application, *Angew. Chem., Int. Ed.*, 2007, **46**(8), 1222–1244.

20 A. Ghemes, O. Dragos-Pinzaru, H. Chiriac, N. Lupu, M. Grigoras, D. Shore, B. Stadler and I. Tabakovic, Controlled Electrodeposition and Magnetic Properties of Co35Fe65 Nanowires with High Saturation Magnetization, *J. Electrochem. Soc.*, 2017, **164**(2), D13–D22.

 

21 R. R. Wildeboer, P. Southern and Q. A. Pankhurst, On the reliable measurement of specific absorption rates and intrinsic loss parameters in magnetic hyperthermia materials, *J. Phys. D: Appl. Phys.*, 2014, **47**(495003), 14.

22 B. D. Cullity and C. D. Graham, *Introduction to Magnetic Materials*, John Wiley & Sons, Inc., 2nd edn, 2009.

23 M. P. Morales, S. Veintemillas-Verdaguer, M. I. Montero, C. J. Serna, A. Roig, L. L. Casas, B. Martinez and F. Sandiumenge, Surface and internal spin canting in gamma-Fe2O3 nanoparticles, *Chem. Mater.*, 1999, **11**(11), 3058–3064.

24 M. Darques, L. Piraux, A. Encinas, P. Bayle-Guillemaud, A. Popa and U. Ebels, Electrochemical control and selection of the structural and magnetic properties of cobalt nanowires, *Appl. Phys. Lett.*, 2005, **86**(7), 072508.

25 M. Darques, J. Spiegel, J. De la Torre Medina, I. Huynen and L. Piraux, Ferromagnetic nanowire-loaded membranes for microwave electronics, *J. Magn. Magn. Mater.*, 2009, **321**(14), 2055–2065.

26 S. Morgan, H. Sohn and R. Victora, Use of trapezoidal waves and complementary static fields incident on magnetic nanoparticles to induce magnetic hyperthermia for therapeutic cancer treatment, *J. Appl. Phys.*, 2011, **109**, 07B305.

27 H. Sohn and R. Victora, Optimization of magnetic anisotropy and applied fields for hyperthermia applications, *J. Appl. Phys.*, 2010, **107**, 09B312.

28 K. R. Hurley, H. L. Ring, M. Etheridge, J. J. Zhang, Z. Gao, Q. Shao, N. D. Klein, V. M. Szlag, C. N. Chung, T. M. Reineke, M. Garwood, J. C. Bischof and C. L. Haynes, Predictable Heating and Positive MRI Contrast from a Mesoporous Silica-Coated Iron Oxide Nanoparticle, *Mol. Pharm.*, 2016, **13**(7), 2172–2183.